IEEE Photonics Journal
An IEEE Photonics Society Publication

Open Access

# Broadband Absorption Enhancement in Modified Grating Thin-Film Solar Cell

Volume 9, Number 3, June 2017

**Muhammad H. Muhammad**
**Mohamed Farhat O. Hameed,** ***Senior Member, IEEE***
**Salah S. A. Obayya,** ***Senior Member, IEEE***

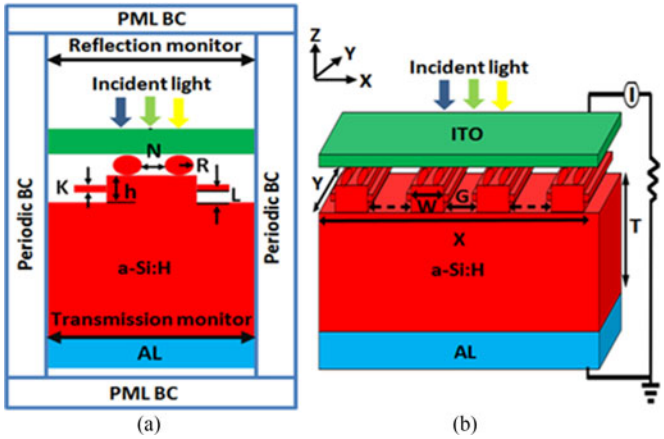


DOI: 10.1109/JPHOT.2017.2698720
1943-0655 © 2017 IEEE

IEEE photonics SOCIETY

IEEE

# Broadband Absorption Enhancement in Modified Grating Thin-Film Solar Cell

**Muhammad H. Muhammad,**[1]
**Mohamed Farhat O. Hameed,**[1,2] ***Senior Member, IEEE*,**
**and Salah S. A. Obayya,**[1] ***Senior Member, IEEE***

[1]Centre for Photonics and Smart Materials, Zewail City of Science and Technology, 6th of October City 12588, Egypt
[2]Mathematics and Engineering Physics Department, Faculty of Engineering, Mansoura University, Mansoura 35516, Egypt

*DOI:10.1109/JPHOT.2017.2698720*


Manuscript received February 15, 2017; revised April 12, 2017; accepted April 23, 2017. Date of publication May 5, 2017; date of current version May 10, 2017. Corresponding author: Salah S. A. Obayya (e-mail: sobayya@zewailcity.edu.eg).

**Abstract:** A novel design of a highly efficient modified grating thin-film solar cell (SC) is reported and analyzed using a 3-D finite difference time domain (3-D FDTD) method. The modified grating has side wings and is covered by 1-D silicon nanorods. The suggested grating has a great potential to harvest the light into the nanoscale active layer. Further, the light trapping through the suggested design is significantly enhanced by the photonic nanorods. The modified grating and nanorods produce an absorption enhancement in different parts of the solar spectrum. Furthermore, the nanorods are considered as a second grating to obtain multiple light trapping which increases the optical path length. Additionally, the nanorods can couple the incident light into the discrete modes of the active layer over an extended wavelength range. Therefore, a broadband absorption enhancement for the suggested SC is achieved. The effects of the structure geometrical parameters on the absorption, ultimate efficiency, and short circuit current of the proposed design are investigated. The performance of the reported SC using crystalline silicon, hydrogenated amorphous silicon, and gallium arsenide is also studied. The numerical results show that high efficiency of 43.114% can be achieved using gallium arsenide with short circuit current density of 35.27 mA/cm$^2$.

**Index Terms:** Grating, photovoltaics, nanorods, finite difference time domain (FDTD) method, thin-film solar cell (TF-SC).

## 1. Introduction

Recently, thin film solar cells (TF-SCs) have an extensive research interest. The TF-SC technology can be used to reduce the cost of the bulk material of photovoltaic devices which paves the road to abundance nature, and low-cost SCs with long term stability [1]. However, the TF-SC is based on polycrystalline or amorphous materials with quite low carrier life time which results in short diffusion length. In order to improve the charge collection efficiency, a relatively thick SC should be used. Therefore, it is required to increase the light absorption while still keeping the active layer thin. This can be achieved by using light trapping techniques to increase the optical path length in a wide range of wavelengths [2], [3]. The light trapping involves the use of random roughness [4], photonic crystals [5], plasmonics [6] and grating structures. The random surface roughness can excite large number of diffraction orders while the ordered gratings excite only a well-defined Fourier spectrum [7]. The theoretical efficiency of such schemes depends on material bandgap [8] and the absorber

thickness [9]. However, the experimentally demonstrated approaches are still below the theoretical lambertian limit [10]. Song *et al*. [11] have studied the optical resonances in laterally oriented Si nanowire arrays. They have achieved short circuit current of 14 mA/cm$^2$ with an enhancement of 60% over the bulk film absorber. Muhammad *et al*. [6] have also reported plasmonic solar cell with 35% absorption improvement compared to the conventional thin film without metallic nano particles. Moreover, the impact of the nanoparticles geometry on the light trapping through TF-SC has been investigated in [12].

The periodic structures such as diffraction grating can achieve better light trapping than random roughness over a limited spectral range. The main objective of the grating is to increase the optical path length to keep the light waves inside the active layer by means of total internal reflection. When the incident light falls normal to the surface of the grating SC, it will pass by anti-reflective coating followed by grating structure. Then, part of the light will be absorbed by the active region of the SC and hence generating electric current. The light will be reflected when it reaches the bottom surface due to the presence of the metallic back reflector. The light will be reabsorbed by the active region of the SC and the photons will have multiple reflections inside the grating grooves which increases the optical path length and hence the absorption [13]. Chang *et al.* [13] have presented a solution to combine micro- and nano-scale surface textures to increase light harvesting in the near infrared for crystalline silicon photovoltaics. The nanostructured ITO anti-reflection layer achieves conversion efficiency of 17.1% with an enhancement factor of 15% [13]. Catchpole and Pillai [14] have also presented an absorption enhancement due to scattering by dipoles into silicon waveguides. Further, Kowalczewski *et al*. [15] have investigated light-trapping in thin-film silicon SCs with rough interfaces which offer short circuit current of 25.5 mA/cm$^2$.

In this paper, a novel technologically feasible TF-SC with periodic modified grating is introduced and studied. The proposed concept of our design is a general way of controlling light based on tailoring of the Fourier components of periodic structures. The simulation results are obtained using the 3-D finite differential time domain (3-D FDTD) via Lumerical software package [16]. The suggested grating has side wings that can enhance light guidance through the active layer. Additionally, one dimensional nano-rods are placed on the modified grating along the active layer surface. The nano-rods act as a second grating that can be used for multiple light trapping to increase the optical path length. Furthermore, the coupling with the supported quasi-guided optical modes results in absorption enhancement. In this study, the role of the grating and nano rods and their impacts on the absorption enhancement are investigated. It is found that each component produces absorption enhancement in a specific part of the solar spectrum. This will lead to a broadband absorption enhancement for the whole device. Carefully engineered structure geometry is proved to offer light absorption enhancement useful for solar cell applications. The reported design offers high efficiency of 39.34%, 42.46%, and 43.114% when crystalline silicon (c-Si), hydrogenated amorphous silicon (a-Si: H), or gallium arsenide (GaAs) are used as active layers, respectively. The achieved ultimate efficiencies are greater than 39.6% and 21.3% reported in [2], and [17], respectively. Further, short circuit current density is enhanced to 32.19, 34.752, and 35.27 mA/cm$^2$ using c-Si, a-Si:H or GaAs as active layers with modified grating and nano-rods.

## 2. Design Considerations

Fig. 1 shows the cross section of a unit cell and 3-D diagram of the reported modified grating TF-SC. The reported SC has an active material of hydrogenated amorphous silicon (a-Si:H) with thickness T, length X, and width Y. Additionally, periodic diffraction grating with wings of the same material is placed on the top surface of the active layer where diffraction of light occurs. The distance between two adjacent gratings is G while, the height and the thickness of the grating wings are L and K, respectively. Further, the width and the height of the gratings are W and h, respectively. Furthermore, 1-D (a-Si:H) cylindrical nano-rods are placed on the nano-grating to obtain high absorption enhancement. The nano-rods of radius R are placed on the grating surface with a distance N between two successive nano-rods. Finally, the active layer with modified grating and nano-rods is coated by ITO layer and is placed over the Al layer.

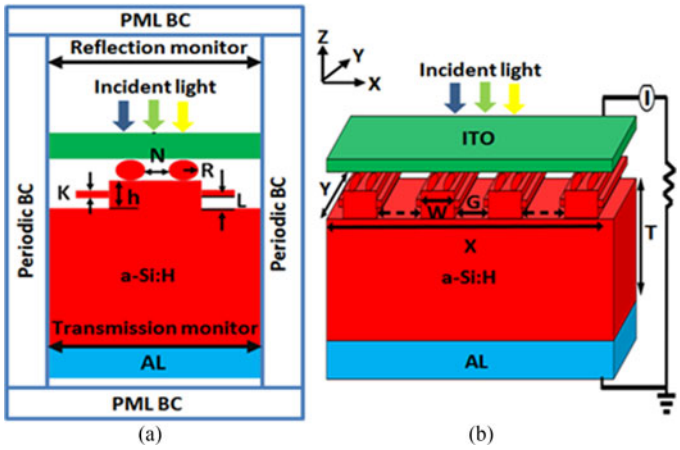


Fig. 1. (a) Two-dimensional side view of a unit cell and (b) 3-D diagram of the proposed modified grating SC with nano-rods.

## 3. Fabrication Techniques

The suggested design is based on grating solar cell which is widely fabricated in the literature [2], [3], [12]. Therefore, the reported design can be investigated according to the following steps. The a-Si:H thin film layer can be formed on a glass carrier by plasma enhanced chemical vapor deposition (PECVD) procedure [12]. The grating structure is then patterned using conventional lithographic and dry etching techniques via e-beam lithography as previously reported in [12]. In order to have an ultra-broadband absorption through the suggested design, nanorods and side arms have been used. It should be also noted that that there is a dramatic improvement in the fabrication techniques of complex solar cell structures. In this regard, Liu *et al.* [18] have fabricated hierarchical structure based on ZnO-NW arrays on Si micro pyramids, as an effective anti-reflection coating (ARC) for improving the energy-conversion efficiency. Further, Singh *et al.* [19] have introduced vertical Si NWs array over three-dimensional micro-pyramid silicon substrate through silver (Ag)-assisted electrolysis wet chemical etching in aqueous hafnium florid (HF) and $AgNO_3$ solution. Moreover, light trapping through thin film has been enhanced using photonic dual grating nanostructures [12]. The dual grating structure shows an appreciable improvement over single gratings patterned either on the top or bottom of the film.

Based on the previously fabricated complex structures, side arms have been added to the suggested modified grating solar cell to obtain ultra-broadband absorption. The side arms can be experimentally fabricated as reported by Jiang *et al.* [20]. Further, Wang *et al.* [21] have presented the solution based technique for branched nanostructures with controlled diameter of identical arms. Moreover, branched nano arms can be formed by vapor transport and condensation during growth as presented in [20] and [21]. Furthermore, a general approach that can control the synthesis of branched and hyper branched nano arms structures has been investigated in [21]. Wang *et al.* [21] can control the nanocluster diameter and density by using a multistep nano-cluster-catalyzed vapor-liquid-solid (VLS) growth process. Further, the nano-rods can be deposited on the grating surface as introduced in [11]. In this regard, scalable processing methods such as chemical vapor deposition (CVD) can be used to grow nanowires on cheap substrates over large areas with reduced manufacturing cost. Additionally, different mechanisms can be used to fabricate silicon nano-wire (SiNWs) [19] such as bottom-up growth mechanisms and top-down etching processes. While growing of SiNWs normally is conducted by using the vapor-liquid-solid (VLS) mechanism, which needs high temperatures, toxic gases and expensive vacuum equipment, top-down etching can be performed in easier ways. It is worth noting that the physical or dry etching is usually conducted in reactive gases through the reactive ion etching process. However, the chemical etching relies on wet chemistries based on hydrofluoric acid for silicon based solar cells. Further, the wet-chemical (WC) etching

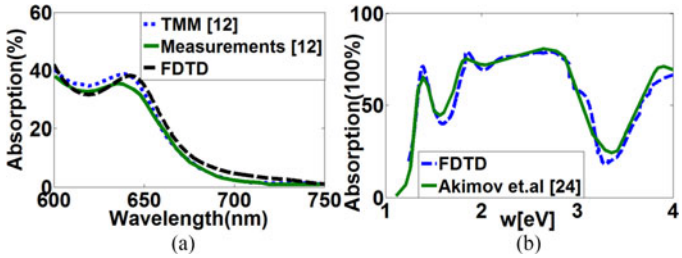


Fig. 2. Wavelength dependent absorption characteristics of (a) dual grating SC [12] and (b) plasmonic SC [25].

is fast and has advantages in terms of cost-effectiveness for mass production. Therefore, it is believed that the suggested design can be experimentally fulfilled.

## 4. Numerical Approach

In this study, the 3-D-FDTD method [16], [22] is applied to calculate the transmission, reflection, and absorption of the proposed modified grating SC. In order to prove the high accuracy of the optical data and simulation technique that are used in our study, the following two validations have been done. Firstly, the dual grating solar cell reported in [12] has been studied by the 3-D-FDTD via Lumerical software package [16]. It is worth noting that Schuster *et al*. [12] have used the transfer matrix method (TMM) to calculate the absorption through the dual grating design. The studied grating solar cell has a:Si layer of thickness 400 nm and 2D dual gratings with a periodicity of 300 nm for both sides. Further, the heights of the upper and lower gratings are equal to 80 nm and 60 nm, respectively. Fig. 2(a) shows the wavelength dependent absorption calculated by the FDTD and that reported experimentally by Schuster *et al.* [12]. Further, the calculated absorption by the TMM [12] is also included in Fig. 2(a). It may be seen from this figure that a good agreement between our results and that obtained from the experimental measurements and the TMM results. The types of the glass or the glue (refractive index) that have been used in the studied grating SC are not clarified in [12] which may cause the slight difference between the 3-D-FDTD and those reported by Schuster *et al.* [12]. Additionally, from modeling point of view, the TMM has some limitations particularly in calculating the proper set of modes (guided and radiated). Unlike the FDTD which solves for the "whole" field, the TMM can sometimes show little discrepancy due to its limitations. Further, the FDTD is different than the TMM in terms of different physical concepts and assumptions [23].

It is worth noting that the reported design is based on hydrogenated amorphous silicon (a-Si:H) whose optical data has been extracted from that reported by Akimov *et al.* [24]. In order to prove the high accuracy of the used optical data, the plasmonic solar cell based on hydrogenated amorphous silicon has been studied and compared to that investigated in [24]. In this study, the optical absorption of a-Si:H solar cell with photo-active layer of thickness 240 nm is calculated as shown in Fig. 2(b). Further, an ITO layer of thickness 20 nm is used as a coating layer with 80 nm thickness of Al back contact. Additionally, metallic nano-particles of radius 10 nm have been placed over the ITO layer as a plasmonic material. It may be seen from Fig. 2(b) that a good agreement is achieved between our results and that reported in [24] which ensures the high accuracy of the used optical data.

Next, the suggested design has been studied using the 3-D-FDTD method [16], [22]. The incident plane wave has an electric field linearly polarized along the x-axis and is normal to x-y plane as revealed from Fig. 1(a). The reported design with only one grating is studied due to the symmetry of the structure. In this case, periodic boundary condition (BC) in x and y- directions are applied with perfect matched layer (PML) BC in z- direction to eliminate unnecessary reflections at the top and bottom boundaries of the simulated unit cell. The multiple scattering caused by grooves, slits, and nano-rods interactions are taken into account using the BCs. Two frequency domain monitors are

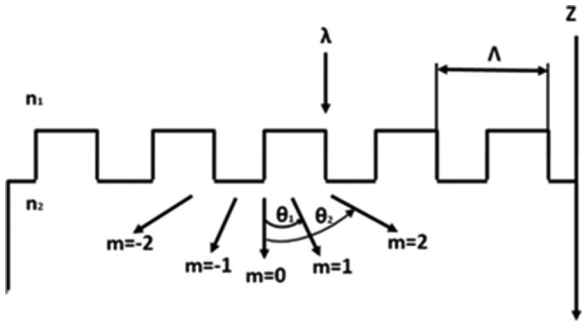


Fig. 3. Schematic diagram of surface diffraction by 1-D surface grating.

also placed above and below the unit cell to calculate the reflection R(λ) and the transmission T (λ), respectively as shown in Fig. 1(a). The meshing parameters and the positions of the source and monitors are first studied to obtain convergent absorption. In this study, the computational domain is taken as 200 nm, 200 nm, and 1090 nm in x, y, and z directions, respectively. Further, non-uniform meshing with minimum cell size of $\Delta x = \Delta y = \Delta z = 0.5$ nm are used to obtain accurate results. Moreover, the source, and reflection monitor are placed above the ITO layer by 390 nm and 400 nm, respectively. However, the transmission monitor is placed above the Al layer as shown in Fig. 1(a). The absorption of the active layer can then be calculated as follows:

$$A(\lambda) = 1 - R(\lambda) - T(\lambda). \tag{1}$$

It is assumed that each absorbed photon produces one electron-hole pair without recombination losses. Therefore, the ultimate efficiency ($\eta$) can be used to evaluate the absorption capability of the proposed solar cell as given by [25]

$$\eta = \frac{\int_{300\text{ nm}}^{\lambda_g} F_s(\lambda)\, A(\lambda) \frac{\lambda}{\lambda_g} d\lambda}{\int_{300\text{ nm}}^{4000\text{ nm}} F_s(\lambda) d\lambda} \tag{2}$$

where $\lambda$ is the wavelength of the incident light, $\lambda_g$ is the bandgap wavelength of the active layer, and $F_s(\lambda)$ is the photon flux density in the ASTM AM 1.5 solar spectrum. The short circuit current density $J_{sc}$ of the proposed design can be calculated by

$$J_{sc} = \eta \frac{e\lambda_g}{hc} \int_{300\text{ nm}}^{4000\text{ nm}} F_s(\lambda)\, d\lambda = 81.83\eta\ (\text{mA/cm}^2). \tag{3}$$

It is worth noting that the ultimate efficiency $\eta$ is related to the short circuit current density Jsc by assuming perfect carrier collection efficiency. This means that each absorbed photon with higher energy than the bandgap results in one electron-hole pair. Consequently, all generated carriers are collected.

## 5. Results and Discussion

### 5.1 Surface Diffraction

The suggested design has a modified grating structure in order to enhance the absorption through the active layer. Therefore, the diffraction effects of the reported design are studied and compared to the conventional grating SC.

Fig. 3 shows a schematic diagram of the conventional 1-D grating SC design. As the incident light reaches the solar cell's grating surface, it will penetrate the cell at specific diffraction angles. The diffraction angle $\theta_m$ depend on the diffraction order, as shown in Fig. 3, the diffraction orders can be calculated for the 1-D surface grating using the following equation:

$$n_2 \sin\theta_m = n_1 \sin\theta_i + m\frac{\lambda}{\Lambda} \tag{4}$$

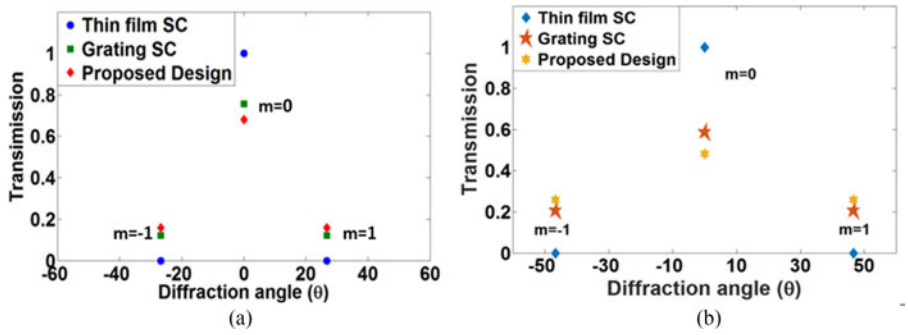


Fig. 4. Fraction of the transmitted power to each physical grating order at different wavelengths. (a) $\lambda = 450$ nm and (b) $\lambda = 650$ nm.

TABLE 1
Shows the Transmitted Light Fraction of the Different Orders at $\lambda = 350$ nm and $\lambda = 650$ nm

| Design | | $\lambda = 450$ nm | | | $\lambda = 650$ nm | | |
|---|---|---|---|---|---|---|---|
| | Grating Orders | m = +1 | m = 0 | m = +1 | m = −1 | m = 0 | m = −1 |
| | Theta ($\theta$) | 26.69° | 0° | −26.6° | 46.6° | 0° | −46.6° |
| Thin film SC | | 0 | 1 | 0 | 0 | 1 | 0 |
| Grating SC | | 0.1215 | 0.7567 | 0.1215 | 0.206 | 0.586 | 0.206 |
| Proposed SC | | 0.159 | 0.681 | 0.159 | 0.258 | 0.482 | 0.258 |

where $n_1$ and $n_2$ are the refractive indices of the first and second mediums, respectively. Additionally, $\theta_i$ represents the angle of incidence; $\Lambda$ is the grating spacing; $\lambda$ is the wavelength; and m is the diffraction order with values of 0, ±1, ±2, etc. Moreover, the reflection from the surface, is known as backward diffraction and a similar expression can be obtained. For 2-D Si gratings surrounded by air, the diffraction angles can be expressed as

$$n_{Si} \sin\theta_{mn} \cos\phi_{mn} = m\frac{\lambda}{\Lambda_x} \tag{5}$$

$$n_{Si} \sin\theta_{mn} \sin\phi_{mn} = m\frac{\lambda}{\Lambda_y} \tag{6}$$

where $\theta_{mn}$ and $\varphi_{mn}$ are the diffraction polar angle and the azimuthal angle at the diffraction order of (m, n), respectively. It should be noted that the diffraction angles are basically independent of the grating depth, d [26].

In this study, the forward (transmission) diffraction for each diffraction order of the suggested modified grating design is calculated using the FDTD Lumerical software package [16]. Fig. 4(a) and (b) shows the fraction of the transmitted power of each physical grating order of the thin film SC, grating SC and the suggested modified grating design at $\lambda = 450$ and 650 nm. It may be noted from this figure that most of the transmitted light is distributed between m = 0, ±1 orders. At m = ±1, the light is propagated through the active layer at oblique angles. Further, the transmitted powers at higher orders increase by increasing the wavelength as may be seen from Table 1 and

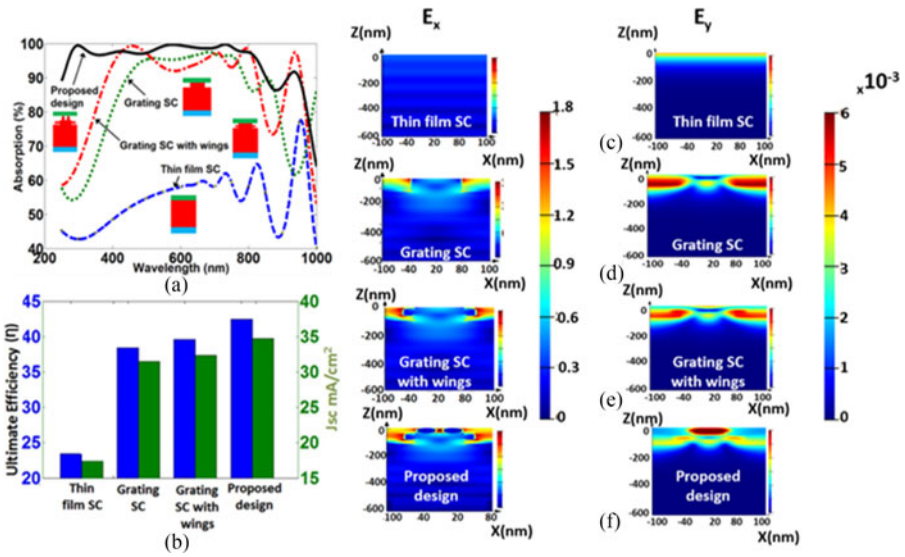


Fig. 5. (a) Wavelength dependent absorptions of thin film SC, grating SC, grating SC with wings, and proposed design with nano-rods. (b) Ultimate efficiency $\eta$ and short circuit current Jsc of the studied designs. Steady-state field distributions along x-z plane of $E_x$ and $E_y$ components at wavelength $\lambda = 460$ nm in (c) conventional SC without grating, (d) grating SC, (e) grating SC with wings, and (f) proposed SC.

Fig. 4. Therefore, the light path and hence the light absorption in the active layer will be increased as shown in Fig. 4(a) and (b).

### *5.2 Modified Grating Design*

Fig. 5(a) and (b) show the absorption variation with the wavelength and corresponding ultimate efficiency and short circuit current density of the conventional thin film SC, grating SC, grating SC with wings and our proposed structure with modified grating and nano-rods. Further, the steady state field profiles of $E_x$ and $E_y$ components in z-direction through the different structures are shown in Fig. 5(c)–(f) at $\lambda = 600$ nm. In this investigation, the photoactive layer is based on hydrogenated amorphous silicon (a-Si:H) of thickness $T = 430$ nm while the thickness of the anti-reflective coating ITO is equal to 20 nm to reduce the surface reflections. Further, the Al layer of thickness 80 nm is used as a back reflector to reduce the transmission through the photovoltaic SC. The grating structure is also made of a-Si:H of height $h = 80$ nm and width $W = 94$ nm with a distance $G = 104$ nm between two adjacent gratings. It is worth noting that the initial dimensions of the suggested design have been chosen based on the conventional grating SC reported in [12]. It has been noted that low absorption was achieved using the conventional grating SC design at short wavelength, as shown in Fig. 5. In order to increase the absorption in such wavelength range, side wings are added to the modified grating. This means that the grating structure is etched from the active layer so that the absorbing material decreases. However, the absorption enhancement increases due to the diffraction effects. The initial dimensions of the side wings are chosen according to the recent fabrication feasibility. The suggested modified grating has side wings of length $= 20$ nm, $K = 20$ nm, and $L = 60$ nm. In order to further increase the absorption of the suggested design, nano-rods are placed over the grating design as shown in Fig. 1. The distance N between two successive nano-rods of radius 20 nm is equal to 30 nm. The length and width of the simulated unit cell shown in Fig. 1(a) are equal to 200 nm. Consequently, the thickness and weight of the photovoltaic cell will be reduced due to reduced amount of manufacturing SC material. Therefore, the cost per watt of output power is ultimately reduced. In this investigation, a parametric study for the geometrical parameters is made to increase the absorption in the active layer and hence the ultimate efficiency.

The effect of a specific parameter is investigated while the other parameters are kept constants at their optimum values.

Fig. 5(a) reveals that the absorptions of the grating SC with and without side wings are greater than that of the conventional thin film SC. Additionally, the absorption of the suggested design with modified grating and nanorods is greater than the grating SC only. The reported design supports multiple reflections of the photons inside the grooves and between the nanorods i.e. (each groove or slit act as a source of light). Therefore, the optical path length and the absorption inside the active layer are increased. Consequently, the a-Si:H structure has multiple total internal reflections which improve the light trapping inside the active layer. Additionally, the reflected light from the surface of the substrate can be absorbed by the grating or wings instead of reflecting it back. Further, the nano-rods act as a grating deposited on the surface of a rectangular grating i.e. (dual grating). The dual grating is used to have multiple light trapping and to couple the incident light into the discrete modes of the thin absorbing layer over an extended wavelength and angular range. Furthermore, the nano-rods produce absorption enhancement in a different part of the solar spectrum than that produced by the grating structure. This will lead to a broadband absorption enhancement over the conventional TF-SC as shown in the field plots of Fig. 5 at $\lambda = 600$ nm. However, the grating surface causes some reflection and hence the active layer absorption percentage is less than 100%. It is also revealed from Fig. 5(b) that the proposed design achieves an overall enhancement for short circuit current density and ultimate efficiency over the conventional thin film SC and grating SC. Additionally, the suggested design has a short circuit current density of 34.752 mA/cm$^2$ which is greater than 19.73 mA/cm$^2$ and 31.466 mA/cm$^2$ of the conventional thin film and grating SCs, respectively. The achieved ultimate efficiencies are greater than 39.6% and 21.3% reported in [2], and [17], respectively. Moreover, the Jsc of the proposed design is greater than 25.5 mA/cm$^2$ that introduced in [14]. Further, the total enhancement of the modified grating SC violates that presented in [13]. Chang *et al.* [13] have presented a solution to combine micro- and nano-scale surface textures to increase light harvesting in the near infrared for crystalline silicon photovoltaics. The nanostructured ITO anti-reflection layer achieves conversion efficiency of 17.1% with an enhancement factor of 15% [13].

It is worth noting that the calculated harvesting efficiency is based on the optical (ultimate) efficiency shown in equation (2). The ultimate efficiency $\eta$ is defined as the maximum efficiency of a photovoltaic cell as the temperature approaches 0 K when each photon with energy greater than the bandgap produces one electron-hole pair as reported in [24] and [27]. It is also worth noting that Huang *et al.* [28] have shown that the maximum theoretical ultimate efficiency of silicon SC is equal to 49.6%. Therefore, the suggested design with ultimate efficiency of 43.114% does not exceed the theoretical limit. However, Shockley Queasier efficiency (power conversion efficiency) is the fraction of the incident power which is converted to electricity. Therefore, the ultimate efficiency can violate the Shockley Queasier limit [30] as reported in [2], [27] and [29]. In this regard, ultimate efficiencies of 39.6%, 39.3%, and 39.9% have been introduced in [2], [27], and [29], respectively, which exceed the Shockley Queasier limit of 33.7%.

Fig. 6(a) and (b) show the absorbed field of the $E_x$ components along x-y plane in the active layer of the conventional and grating TF-SC, respectively. In addition, the absorbed fields in the grating SC with wings and the suggested design with nano-rods are plotted in Fig. 6(c) and (d), respectively. It may be seen from Fig. 6 that the modes are strongly confinement around the grating or in the grooves between gratings and between nano-rods. Therefore, the light trapping through the active layer is increased with reduced reflection. Consequently, the absorption through the active layer of the reported design is better than those of the grating SC with and without wings. This is confirmed by the filed plots in z-direction shown in Fig. 5. Furthermore, the absorption exceeds 90% over wide band of wavelengths as shown in Fig. 5. It should be also noted that the peak and valley shown in Fig. 5 around $\lambda = 900 \sim 930$ nm and $\lambda = 800 \sim 870$ nm are due to the Fabry–Perot cavity resonance within the a-Si:H active layer. Moreover, the other absorption peaks and valleys are resulted from constructive and destructive interference. The effect of the structure geometrical parameters is studied to maximize the light absorption through the suggested design.

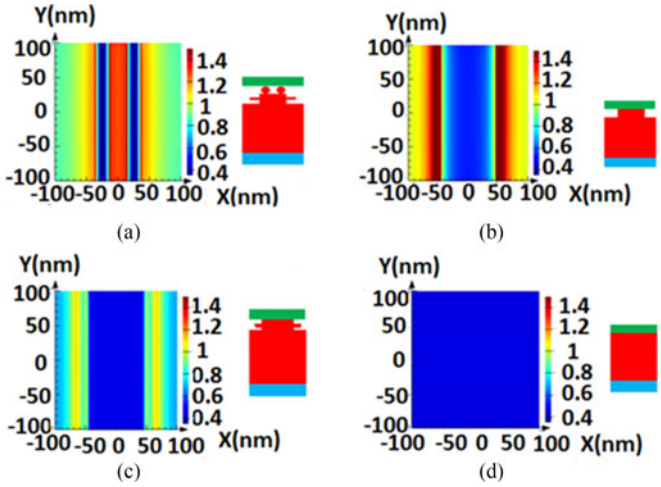


Fig. 6. Steady-state field distributions of $E_x$ components along x-y plane at wavelength $\lambda = 460$ nm in (a) conventional SC without grating, (b) grating SC, (c) grating SC with wings, and (d) proposed SC.

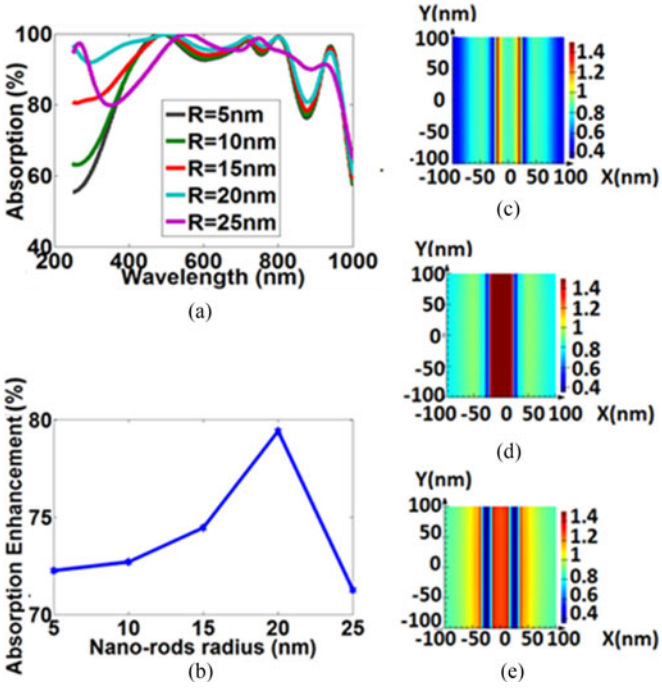


Fig. 7. (a) Spectral absorption as a function of the wavelength at different nano-rods radii R = 5, 10, 15, 20, and 25 nm. (b) Variation of absorption enhancement with nano-rods radius. Absorbed fields along x- y plane of the $E_x$ components at wavelength $\lambda = 300$ nm at different rods radii. (c) R = 5 nm, (d) R = 15 nm. (e) R = 20 nm.

Fig. 7(a) shows the wavelength dependent photoactive layer absorption % of the reported structure at different nano-rods radii. The figure reveals that the absorption increases as the radius of the rods increases from R = 5 nm to R = 20 nm due to the strong confinement of the light between the nano-rods as evident in Fig. 5(c)–(e). These figures show the field distributions along x-y plane of the $E_x$ components at $\lambda = 300$ nm at R = 5 nm, 15 nm and 20 nm. If the nano-rods radius is further increased, the reflection increases, and hence, absorption decreases, as shown in Fig. 7(b). Fig. 7(b) shows the absorption enhancement as a function of nano-rods radius. At R = 20 nm, maximum absorption enhancement of 79.42% can be achieved over conventional thin film SC. The

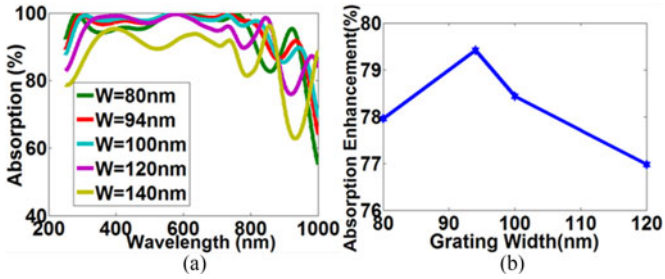


Fig. 8. Spectral absorption as a function of the wavelength at different grating widths W = 80, 94, 100, 120, and 140 nm. (b) Variation of the absorption enhancement with the grating width.

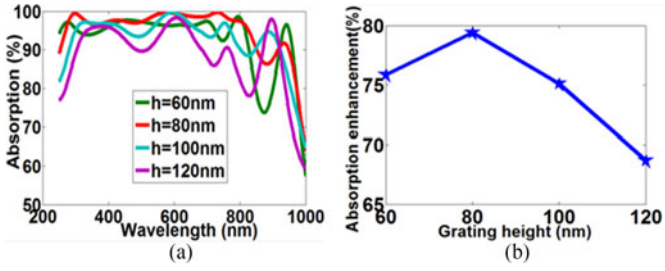


Fig. 9. Wavelength dependent spectral absorption at different grating heights h = 60, 80, 100, and 120 nm. (b) Variation of the absorption enhancement with the grating height.

total enhancement of the optical power absorption E% is calculated by using the total absorbed power $P_{total}$ of the proposed design, and the total absorbed power $P_{total}$ of the conventional TF-SC without grating as follows [1]:

$$E\% = \frac{P_{total}\,(\text{proposed design})}{P_{total}\,(\text{conventional TF–SC})} - 1. \tag{7}$$

The total absorbed powers are calculated by integrating the absorption rate of the photoactive layer. It is found that the grating a-Si:H SC without wings or nano-rods offers 66.7% absorption enhancements over the conventional TF-SC. However, the proposed design achieves 79.42% absorption enhancement.

Fig. 8(a) shows the spectral absorption at different grating widths while the grating height and nano-rods diameter are taken as in 80 nm and 20 nm, respectively. Additionally, the absorption enhancement as a function of the grating width is shown in Fig. 8(b). It is revealed from Fig. 8(a) that the absorption increases by increasing the grating width from 80 nm to 94 nm. If the grating width is further increased, the surface area of the (a-Si:H) grating, and hence, the reflection will be increased. Consequently, the absorption and absorption enhancement through the active area will be decreased as shown in Fig. 8. The effect of the grating height is next studied.

Fig. 9 shows the variation of the absorption percentage % of the photovoltaic active layer at different grating heights h = 60, 80, 100, and 120 nm while the width of the grating is fixed at W = 96 nm. Further, the variation of the absorption enhancement with the grating height is shown in Fig. 9(b). It is evident from Fig. 7 that maximum absorption, and hence, absorption enhancements are achieved at height of 80 nm.

The tolerances of the nano-rods radius and the grating height and width are also investigated. It is worth noting that the tolerance of a specific parameter is calculated while the other parameters of the proposed design are kept constants at their optimum values. It is found that the grating height and width and nano-rods radius allow a tolerance of 5% at which the ultimate efficiency are still better than 42%.

TABLE 2
Optimum Parameters of the Suggested Modified Grating Thin Film SC

| Parameter | Value (nm) | Parameter | Value (nm) |
|---|---|---|---|
| W | 94 | N | 30 |
| G | 106 | X | 200 |
| h | 80 | Y | 200 |
| K | 20 | Z | 550 |
| L | 60 | T | 550 |
| R | 20 | | |

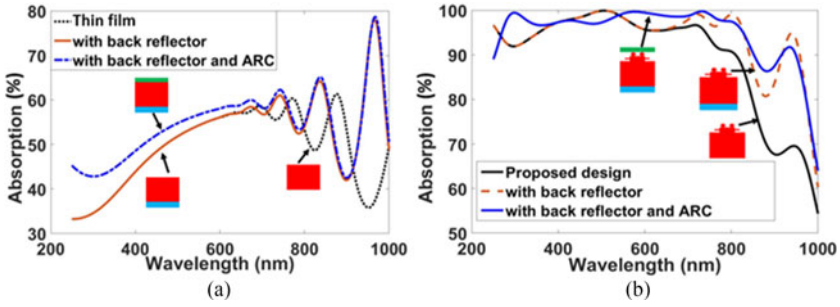


Fig. 10. (a) Wavelength dependent absorptions of thin film only, with back reflector and with back reflector and ARC, and (b) wavelength dependent absorptions of the proposed design only, with back reflector and with back reflector and ARC

The effects of the anti-reflection coating (ARC) and back reflector on the absorption of the suggested SC are also studied. Table 2 shows the optimum dimensions of the proposed structure. Fig. 10(a) shows the absorption curve for thin film solar cell without grating structure. Also, the wavelength dependent absorptions of thin film solar cell with back reflector with/without antireflection coating are also shown in this figure. It may be seen from the figure that at short wavelength, the ARC has a dominant effect that can increase the absorption through the active layer of the solar cell. Further, the use of ARC along with back reflector enhances significantly the absorption through the active layer at longer wavelength. Fig. 10(b) shows the impact of the ARC and back reflector on the absorption of the suggested thin film solar cell with modified grating design. It may be seen from this figure that the proposed modified grating design improves the absorption in the short wavelength region compared to thin film only shown in Fig. 10(a). Therefore, the short wavelength spectrum is highly absorbed due to the modified grating of the solar cell, since silicon exhibits a high absorption coefficient for shorter wavelengths. However, the longer wavelength region can be absorbed by using additional structure help. In this regard, back reflector has been used to increase the light trapping and the power absorption in the silicon layer. Therefore, interferences between the forward and backward propagating waves occur through the active layer and hence an absorption enhancement is achieved as shown in Fig. 10(b). Further, spatial resonance of optical wave occurs due to the presence of both diffraction conditions by surface texturing and reflection by back reflector which are met simultaneously within narrow bandwidth and limited incident angles. Therefore, the usage of the anti-reflection coating and back reflector can play a vital role in the absorption of the long wavelength. Since a diffraction grating with the proposed design results in a gradual change of refractive index compared to a rectangular groove grating, it provides better anti-reflection and, hence, larger $J_{SC}$, compared to thin film SC structure.

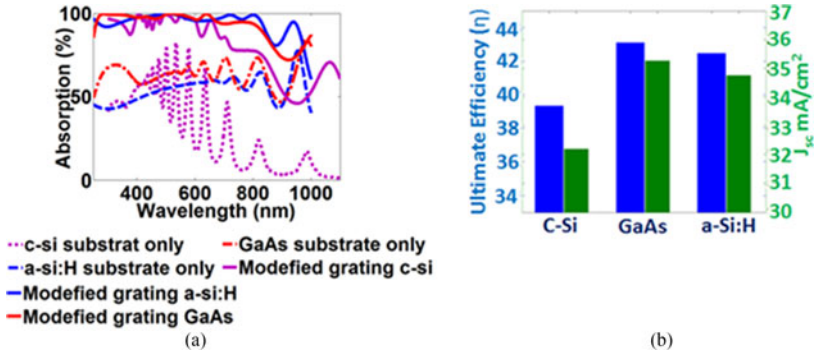


Fig. 11. (a) Spectral absorption of the photo-active layer of the proposed design and conventional TF-SC at different materials c-Si, a-Si:H, and GaAs. (b) Ultimate efficiency $\eta$ and short circuit current $J_{sc}$ calculated as a function of the photoactive layer material type.

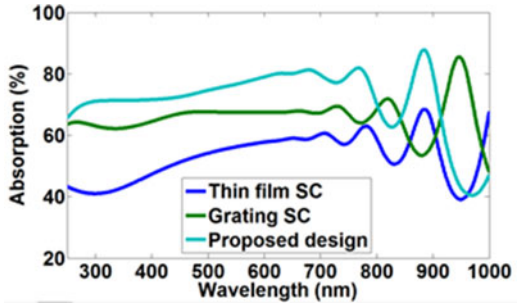


Fig. 12. Spectral absorption of the photo-active layer of the proposed design, Grating SC, and conventional TF-SC using y-polarized incident plane wave.

The effect of the material type of the photoactive layer is also investigated. Fig. 11(a) shows the spectral absorption of the photoactive layer of the proposed design and conventional TF-SC based on GaAs [31], a-Si:H [24] and c-Si [32]. It is evident from Fig. 11(a) that great enhancement occurs in the absorption of the proposed design over the conventional TF-SC in all studied cases over a wide range of wavelength. The numerical results reveal that 178.7%, 79.42% and 50.4% absorption improvements are achieved by using c-Si, a-Si:H, or GaAs, respectively, over the corresponding conventional TF-SCs without grating. This is due to the good confinement of the mode around the modified grating with wings and the modified light trapping through the active layer. Therefore, the optical path length and hence the absorption through the active layer are increased which is vital for SC based on indirect bandgap materials. It is also evident from Fig. 11 that the absorptions of the GaAs and a-Si:H photoactive layers of the proposed design are greater than that with c-Si material specially for long wavelength. Fig. 11(b) shows the ultimate efficiency and the short circuit current as a function of the active material type. The suggested design with photoactive layer of c-Si, a-Si:H, and GaAs have high ultimate efficiency of 39.34%, 42.46%, and 43.114%, respectively. Additionally, the short circuit current densities Jsc of the corresponding designs are improved to 32.19, 34.752, and 35.27 mA/cm$^2$. It is worth noting that the achieved efficiency of the proposed design using GaAs of 43.114% is higher than that reported in [2], [12], [27] and [33]. Additionally, the suggested design has an ultra-broadband absorption over wide range of wavelengths compared to the absorption investigated in [2], [12], [27], [33], [34]. Further, the achieved short circuit current density of 35.27 mA/cm$^2$ is greater than that presented in [35]–[40].

Finally, the effect of the polarization of the incident plane wave on the performance of the suggested design is finally investigated. Fig. 12 shows the absorption spectra using the incident y-polarized plane wave for thin film SC, grating SC and modified design with nano-rods and side wings. It may be shown from this figure that the proposed design offers an absorption enhancement

relative to the thin film SC and the conventional grating SC. Further the ultimate efficiency of the studied design are equal to 24.362%, 29.0885% and 33.0166%, respectively. It is worth noting that the absorption of the y-polarized plane wave is less than that of the incident x-polarized case. This is due to the configuration of the grating design which has more index variation in x-direction than that in y-direction. Therefore the absorption enhancement due to the diffraction effect in x-direction is better than that occurs in y-direction.

## 6. Conclusion

The absorption enhancement of TF-SC by using modified grating with nano-rods is studied using 3-D-FDTD method. We identify the mechanism used to calculate the absorption, short circuit current and ultimate efficiency of the proposed design. Additionally, the influences of nano-rods, grating size, and material type are considered in order maximize the absorption enhancement of the suggested SC. The grooves arrays with nano-rods offer considerable increase in the absorption of the photoactive layer. The suggested design based on the GaAs as an active material shows maximum efficiency of $\eta = 43.114\%$ compared to the other different materials with $J_{sc} = 35.27\,mA/cm^2$.

## References


[1] C. Lundgren, R. Lopez, J. Redwing, and K. Melde, "FDTD modeling of solar energy absorption in silicon branched nanowires," *Opt. Exp.*, vol. 21, pp. A392–A400, 2013.

[2] F. N. Rahman, M. I. Khalil, T. Latif, and M. A. Haque, "Performance enhancement of thin-film c-Si solar cell with group III-V material grating structures," in *Proc. IEEE Jordan Conf. Appl. Elect. Eng. Comput. Technol.*, Amman, Jordan, 2013, pp. 1–5.

[3] E. R. Martins, J. Li, Y. Liu, J. Zhou, and T. F. Krauss, "Engineering gratings for light trapping in photovoltaics: The super cell," *Phys. Rev.*, vol. 86, pp. 041404-1-041404-4, 2012.

[4] P. Kowalczewski, M. Liscidini, and L. C. Andreani, "Engineering Gaussian disorder at rough interfaces for light trapping in thin-film solar cells," *Opt. Lett.*, vol. 37, no. 23, pp. 4868–4870, 2012.

[5] L. Zhao, Y. H. Zuo, C. L. Zhou, H. L. Li, H. W. Diao, and W. J. Wang, "A highly efficient light-trapping structure for thin-film silicon solar cells," *Sol. Energy*, vol. 84, no. 1, pp. 110–115, 2010.

[6] M. H. Muhammad, M. F. O. Hameed, and S. S. A. Obayya, "Broad band absorption enhancement in periodic structure solar cells," *Opt. Quantum Electron.*, vol. 47, pp. 1487–1494, 2015.

[7] F. J. Tsai, J. Y. Wang, J. J. Huang, Y. W. Kiang, and C. C. Yang, "Absorption enhancement of an amorphous Si solar cell through surface plasmon-induced scattering with metal nanoparticles," *Appl. Phys. Lett*, vol. 92, 2008, Art. no. 171114.

[8] C. H. Henry, "Limiting efficiencies of ideal single and multiple energy gap terrestrial solar cells," *J. Appl. Phys.*, vol. 51, no. 8, pp. 4494–4500, 1980.

[9] A. Bozzola, M. Liscidini, and L. Andreani, "Photonic light-trapping versus Lambertian limits in thin film silicon solar cells with 1-D and 2D periodic patterns," *Opt. Exp.*, vol. 20, no. S2, pp. A224–A244, 2012.

[10] Z. Yu, A. Raman, and S. Fan, "Fundamental limit of light trapping in grating structures," *Opt. Exp.*, vol. 18, no. S3, pp. A366–A380, 2010.

[11] K. D. Song, T. J. Kempa, H. G. Park, and S. K. Kim, "Laterally assembled nanowires for ultrathin broadband solar absorbers," *Opt. Exp.*, vol. 22, pp. A992–A1000, 2014.

[12] C. S. Schuster *et al.*, "Dual gratings for enhanced light trapping in thin-film solar cells by a layer-transfer technique," *Opt. Exp.*, vol. 21, pp. A433–A438, 2013.

[13] C. H. Chang, M. H. Hsu, W. L. Chang, W. C. Sun, and P. Yu, "Indium-tin-oxide nanowhiskers crystalline silicon photovoltaics combining micro- and nano-scale surface textures," *Proc. SPIE*, vol. 7933, 2011, Art. no. 79332M.

[14] K. R. Catchpole and S. Pillai, "Absorption enhancement due to scattering by dipoles into silicon waveguides," *Appl. Phys.*, vol. 100, 2006, Art. no. 044504.

[15] P. Kowalczewski, M. Liscidini, and L. C. Andreani, "Light trapping in thin-film solar cells with randomly rough and hybrid textures," *Opt. Exp.*, vol. 21, pp. A808–A820, 2013.

[16] [Online]. Available: www.lumerical.com

[17] N. Tucher *et al.*, "Crystalline silicon solar cells with enhanced light trapping via rear side diffraction grating," in *Proc. 5th Int. Conf. Silicon Photovolt., Silicon PV*, 2015, vol. 77, pp. 253–262.

[18] Y. Liu *et al.*, "Hybridizing ZnO nanowires with micropyramid silicon wafers as superhydrophobic high-efficiency solar cells," *Adv. Energy Mater.*, vol. 2, no. 1, pp. 47–51, 2012.

[19] P. Singh *et al.*, "Fabrication of vertical silicon nanowire arrays on three dimensional micro-pyramid-based silicon substrate," *J. Mater. Sci.*, vol. 50, no. 20, pp. 6631–6641, 2015.

[20] X. Jiang *et al.*, "Rational growth of branched nanowire heterostructures with synthetically encoded properties and function," *Proc. Nat. Acad. Sci. USA*, vol. 108, pp. 12212–12216, 2011.

[21] D. Wang, F. Qian, C. Yang, Z. Zhong, and C. M. Lieber, "Rational growth of branched and hyperbranched nanowire structures," *Nano Lett.*, vol. 4, pp. 871–874, 2004.

[22] S. S. A Obayya, M. F. O. Hameed, and N. F. F. Areed, *Computational Liquid Photonics: Fundamental, Modeling and Applications*. New York, NY, USA: Wiley, 2016.

[23] J. B. Chen, Y. Shen, W. X. Zhou, Y. X. Zheng, H. Zhao, and L. Chen, "Comparison study of the band-gap structure of a 1-D-photonic crystal by using TMM and FDTD analyses," *J. Korean Phys. Soc.*, vol. 58, no. 4, pp. 1014–1020, 2011.
[24] Y. Akimov, K. Ostrikov, and E. P. Li, "Surface plasmon enhancement of optical absorption in thin-film silicon solar cells," *Opt. Exp.*, vol. 4, pp. 107–113, 2009.
[25] M. Hussein, M. F. O. Hameed, N. F. F. Areed, and S. S. A. Obayya, "Ultra-high efficient solar cell based on decagonal arrays of silicon nanowires," *Opt. Eng.*, vol. 53, no. 11, pp. 117105-1–117105-8, 2014.
[26] H. Sai, Y. Kanamori, K. Arafune, Y. Oshita, and M. Yamaguchi, "Light trapping effect of submicron surface textures in crystalline Si solar cells," *Progress Photovolt, Res. Appl.*, vol. 15 pp. 415–423, 2007.
[27] S. E. Han, A. Mavrokefalos, M. S. Branham, and G. Chen, "Efficient light-trapping nanostructures in thin silicon solar cells," *Proc. SPIE*, vol. 8031, 2015, Art. no. 80310T.
[28] N. Huang, C. Lin, and M. L Povinelli, "Broadband absorption of semiconductor nanowire arrays for photovoltaic applications," *J. Opt.*, vol. 14, pp. 1–7, 2012.
[29] M. F. O. Hameed, M. Abdelrazzak, and S. S. A. Obayya, "Novel design of ultra-compact triangular lattice silica photonic crystal polarization converter," *IEEE J. Lightw. Technol.*, vol. 31, no. 1, pp. 81–86, Jan. 2013.
[30] J. Grandidier, M. G. Deceglie, D. M. Callahan, H. A. Atwater, and T. J. Watson, "Simulations of solar cell absorption enhancement using resonant modes of a nanos-phere array," in *Proc. SPIE*, vol. 8256, 2012, Art. no. 825603.
[31] X. Wang, M. R. Khan, J. L. Gray, and M. A. Alam, "Design of GaAs solar cells operating close to the Shockley–Queisser limit," *IEEE J. Photovolt.*, vol. 3, no. 2, pp. 737–744, 2013.
[32] Y. Huang *et al.*, "Comparative investigation on designs of light absorption enhancement of ultrathin crystalline silicon for photovoltaic applications," *J. Photon. Energy*, vol. 6, pp. 047001-1–047001-10, 2016.
[33] L. H. Zhu, M. R. Shao, R. W. Peng, R. H. Fan, X. R. Huang, and M. Wang, "Broadband absorption and efficiency enhancement of an ultra-thin silicon solar cell with a plasmonic fractal," *Opt. Exp.*, vol. 21, no. s3, pp. A313–A323, 2013.
[34] S. Hajimirza and J. R. Howell, "Flexible nano texture structures for thin film PV cells using wavelet functions," *IEEE Trans. Nanotechnol.*, vol. 14, pp. 904–910, 2015.
[35] R. Chriki, A. Yanai, J. Shappir, and U. Levy, "Enhanced efficiency of thin film solar cells using a shifted dual grating plasmonic structure," *Opt. Exp.*, vol. 21, no. S3, 2013.
[36] D. A. Goldman, J. Murray, and J. N. Munday, "Nanophotonic resonators for InP solar cells," *Opt. Exp.*, vol. 24, no. 10, pp. A925–A934, 2016.
[37] R. Dewan, M. Marinkovic, R. Noriega, S. Phadke, A. Salleo, and D. Knipp, "Light trapping in thin-film silicon solar cells with submicron surface texture," *Opt. Exp.*, vol. 17, no. 25, pp. 23058–23065, 2009.
[38] M. Hussein, M. F. O. Hameed, N. F. F. Areed, and S. S. A. Obayya, "Ultra-high efficient solar cell based on decagonal arrays of silicon nanowires," *Opt. Eng.*, vol. 53, 2014, Art. no. 117105.
[39] M. Hussein, M. F. O. Hameed, N. F. F. Areed, A. Yahia, and S. S. A. Obayya, "Funnel-shaped silicon nanowire for highly efficient light trapping," *Opt. Lett.*, vol. 41, pp. 1010–1013, 2016.
[40] S. S. A. Obayya, N. F. Fahmy, M. F. O. Hameed, and M. Hussein, "Optical nano-antennas for energy harvesting," in *Innovative Materials and Systems for Energy Harvesting Applications*, M. Luciano, L. Onofrio, and P. Francesco, Eds. Hershey, PA, USA: IGI Global, 2015, pp. 26–62.